Journal of Ceramic Processing Research. Vol. 17, No. 3, pp. 152~155 (2016)

J O U R N A L O F
Ceramic Processing Research

Improved electrochemical performance of hybrid supercapacitor using Zr doped $Li_4Ti_5O_{12}$ anode

Hyeong-Jong Choi[a], Seung-Hwan Lee[a], Hong-Ki Kim[a], Sung-Gap Lee[b], In-Ho Im[c] and Young-Hie Lee[a,*]

[a]*Dept. of Electronic Materials Engineering, Kwangwoon University*
[b]*Dept. of Ceramic Engineering, Eng. Res. Insti., Gyeongsang National University*
[c]*Dept. of Electrical Engineering, Shin Ansan University*

The cylindrical hybrid supercapacitors are fabricated using the activated carbon as the cathode and $Li_4Ti_{5-x}Zr_xO_{12}$ ($0 \le x \le 0.6$) as the anode. The x-ray diffraction patterns of the $Li_4Ti_{5-x}Zr_xO_{12}$ ($0 \le x \le 0.6$) exhibited that Zr entered into the Ti-site and the $Li_4Ti_{5-x}Zr_xO_{12}$ ($0 \le x \le 0.45$) was well-crystallized without secondary phases. This increased lattice parameter and conductivity of $Li_4Ti_5O_{12}$. However excessive Zr doping caused inferior electrochemical performance due to impurity phases. The bigger CV region of $Li_4Ti_{5-x}Zr_xO_{12}$ ($0.15 \le x \le 0.45$) can be inferred that Zr leads more active electrochemical performance than that of $Li_4Ti_5O_{12}$. The Zr also improved the initial charge-discharge capacitance as well as cycling stability. The hybrid supercapacitor using $Li_4Ti_{4.55}Zr_{0.45}O_{12}$ anode shows the most excellent electrochemical performance.

Key words: Cylindrical Hybrid Supercapacitor, Electrochemical Performance, Li4Ti5O12, Activated Carbon, Zr doping.

Introduction

Nowadays, world is faced with continuous exhaustion of energy sources, environmental pollution and natural catastrophes. In order to solve these problems, the energy storage devices have been attracting attention. Recently, energy storage devices have been applied to hybrid electric vehicle (HEV) and energy storage system (ESS). There are many type energy storage devices. Among them, the Li-ion secondary batteries and supercapacitors have been mostly used. The Li-ion secondary batteries provide the high energy density (150-200 $Whkg^{-1}$), advantage of Li-ion secondary batteries. However, Li-ion secondary batteries have a low power density and short cycle life [1-3]. In contrast, the supercapacitors have high power density (10^3-10^4 Wkg^{-1}), long cycle life and low energy density [4-6]. To remedy the above shortcomings, the hybrid supercapacitors were designed. The hybrid supercapacitors incorporate the beneficial properties of both systems. Generally, the hybrid supercapacitors used the cathode materials of supercapacitors and anode materials of secondary batteries. Therefore, hybrid supercapasciors provide high power density, high energy density and long cycle life [7]. The numerous materials are used as the anode of hybrid supercapacitors [8, 9]. Among them, the $Li_4Ti_5O_{12}$ is promising candidate materials for anode. Spinel $Li_4Ti_5O_{12}$ shows zero strain material because spinel $Li_4Ti_5O_{12}$ is near zero change in unit cell volume during insertion and desorption of lithium ions [10]. Therefore, $Li_4Ti_5O_{12}$ has excellent structural stability. The $Li_4Ti_5O_{12}$ is transformed into the rock-salt structure $Li_7Ti_5O_{12}$ [11].

$$Li_4Ti_5O_{12} + 3Li+ + 3e \leftrightarrow Li_7Ti_5O_{12},\ E = 1.5\ V$$

However, spinel $Li_4Ti_5O_{12}$ have disadvantages such as slow Li-ion diffusion coefficient ($< 10^{-12}$ cm^2 s^{-1}) [12] and poor electron conductivity (2.65×10^{-7} S cm^{-1}) [13]. Theses disadvantages limit capacity at high charge-discharge. Therefore, there are needs for improving for Li-ion diffusion coefficient and poor electron conductivity. In order to improve these problems, various methods are proposed such as synthesizing nano-sized particles, the doping of various metal ions [12, 14, 15], non-metal ions [16, 17], coating or mixing with conductive materials [18]. Among these methods, the doping is widely used method. It can improve the electronic conductivity of the $Li_4Ti_5O_{12}$ by substituting a various metal ions on a Ti site [19]. Also, the $Li_4Ti_5O_{12}$ particles size is reduced by doping system [19]. The small particle size of the $Li_4Ti_5O_{12}$ leads to fast Li-ion diffusion because of the shorted Li-ion path and widened electrode/electrolyte contact surface [20, 21]. In this paper, we investigated the electrochemical performance of hybrid supercapacitors using Zr doped $Li_4Ti_5O_{12}$ with different concentrations (0×0.6) as anode and activated carbon as cathode.

Experiments

$Li_4Ti_{5-x}Zr_xO_{12}$ (0x0.6) samples were fabricated using solid-state methods with Li_2CO_3 (Junsei, 99%), TiO_2 (Junsei, 99%), and ZrO_2 (Fluka, 99%) as raw materials.

*Corresponding author:
Fax: +82-2-915-8084
E-mail: yhlee@kw.ac.kr

The powders were mixed in ethyl alcohol for 24 h in a ball mill and calcined at 800 °C for 6 h in air. We used X-ray diffraction (XRD) and field emission scanning electron microscopy (FE-SEM) to analyze the crystallinity and the morphology. The anode was composed of $Li_4Ti_{5-x}Zr_xO_{12}$, conductive carbon black binder (Super P), and polyvinylidene fluoride (PVDF) in the weight ratio 83 : 7 : 10. N-Methyl pyrrolidinine (NMP) as a solvent was added to produce the slurry. The prepared slurry was coated on aluminum foil to a thickness of 125 μm using a bar coater and then dried at 100 °C to remove the NMP solvent. The material was then pressed to a thickness of 70-80 μm. The width of the cathode, separator, and anode were 28 cm, 40 cm, and 30 cm, respectively and the height of the cathode and anode were both 3 cm. The prepared electrodes and separator were assembled into a cylindrical cell (outer diameter of 2 cm × height of 4.5 cm) in an argon-gas-filled glove box. Before being impregnated with a 1.5 M solution of $LiBF_4$ as the electrolyte, the cell was dried in a vacuum oven for 48 h to get rid of the moisture. The galvanostatic charge-discharge tests (initial capacitance, rate capability) were carried out using Arbin BT 2042 battery test system at various current densities with a cut off voltage of 0-2.8 V. The electrochemical impedance spectroscopy (EIS) was done in the frequency range of 10^{-1} to 10^{-6} Hz.

Results and Discussion

Fig. 1 (a) show the x-ray diffraction patterns of the $Li_4Ti_{5-x}Zr_xO_{12}$ ($0 \le x \le 0.6$) to identify crystalline structure. All peaks show similar to the original $Li_4Ti_5O_{12}$ (PDF No, 49-0207) with Fd3m space group (PDF No, 49-0207). No secondary phases were observed until $x = 0.45$ because the Zr is completely entered into the $Li_4Ti_5O_{12}$ structure. However, the some impurity phases were observed by excessive Zr

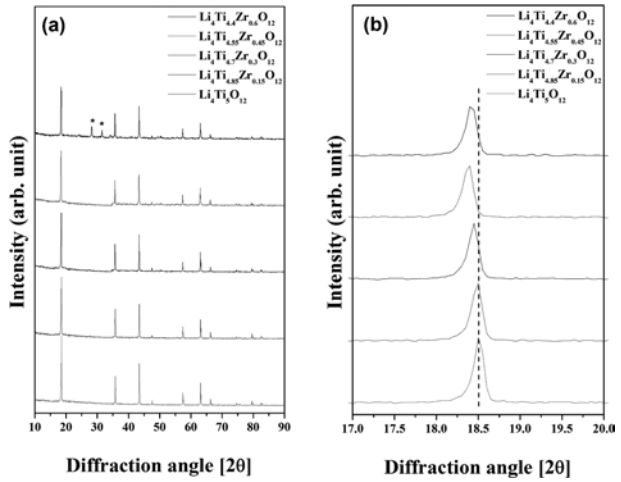

Fig. 1. (a) XRD patterns of the $Li_4Ti_{5-x}Zr_xO_{12}$ ($0 \le x \le 0.6$) powders. (b) Enlarged XRD patterns between 17 and 20 degrees.

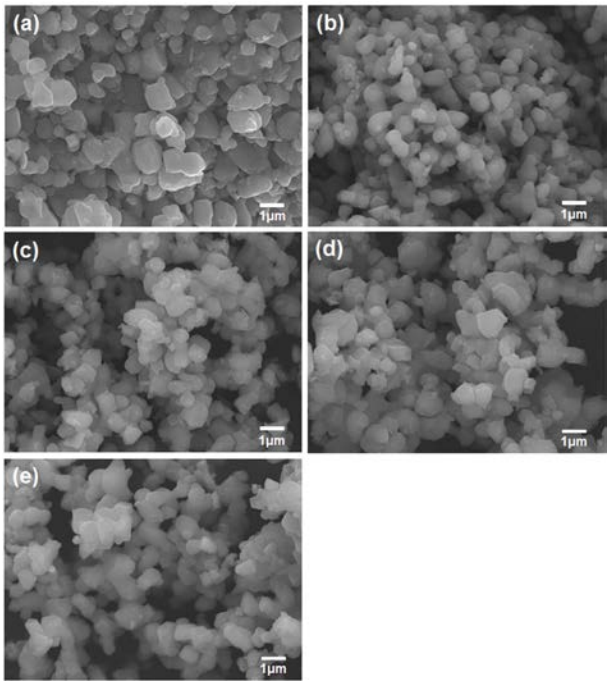

Fig. 2. SEM images of the (a) Pristine $Li_4Ti_5O_{12}$,(b) $Li_4Ti_{4.85}Zr_{0.15}O_{12}$, (c) $Li_4Ti_{4.7}Zr_{0.3}O_{12}$, (d) $Li_4Ti_{4.55}Zr_{0.45}O_{12}$, and (e) $Li_4Ti_{4.4}Zr_{0.6}O_{12}$ powders.

contents at $x = 0.6$. These structural properties were expected to affect electrochemical performance of hybrid supercapacitor. Fig. 1(b) shows the enlarged XRD patterns from 17 to 20 °. All peaks were shifted toward lower degrees with increasing Zr concentration. We can infer that the lattice parameter of samples is proportional to Zr concentration due to smaller radius of Ti (0.605 Å) than that of Zr (0.80 Å) as calculated using Bragg's equation. This also affects the electrochemical performance of hybrid supercapacitor because of length of Li-ion path.

Fig. 2 shows the microstructures of the Zr doped $Li_4Ti_{5-x}Zr_xO_{12}$ and pristine $Li_4Ti_5O_{12}$. All samples show a similar morphology and particle size smaller than 1 um. The Zr doped $Li_4Ti_{5-x}Zr_xO_{12}$ show less particle agglomerations than that of the pristine $Li_4Ti_5O_{12}$. As a result, the particle sizes of Zr doped $Li_4Ti_5O_{12}$ is slightly decreased compared to pristine $Li_4Ti_5O_{12}$. The small particle size leads to enhanced electrochemical performance owing to the shorted Li-ion path and widened electrode/electrolyte contact surface [12, 21, 22].

Fig. 3shows the initial charge-discharge curves of hybrid supercpacitor using the $Li_4Ti_{5-x}Zr_xO_{12}$ anode. We can significantly see that the Zr doped $Li_4Ti_5O_{12}$ show higher capacitance than pristine. With increasing Zr content, the initial charge-discharge gradually increased. This can be explained by improvement of conductivity and structural properties as shown in Fig. (1) and (2). The highest specific capacitance is 69 Fg^{-1} at $x = 0.45$ and on the contrary, the decreasing tendency is shown in more than that. This result is related with decomposition of

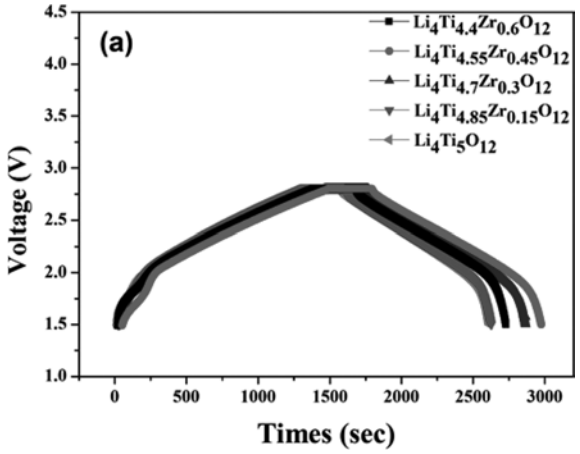

Fig. 3. Initial charge-discharge curves of the hybrid supercapacitors using $Li_4Ti_{5-x}Zr_xO_{12}$ ($0 \le x \le 0.6$) anode materials.

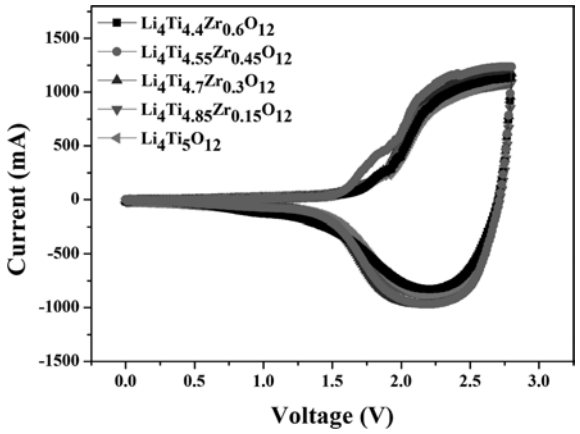

Fig. 4. Cyclic voltammetric (CV) curves of the hybrid supercapacitors using the $Li_4Ti_{5-x}Zr_xO_{12}$ ($0 \le x \le 0.6$) anode materials.

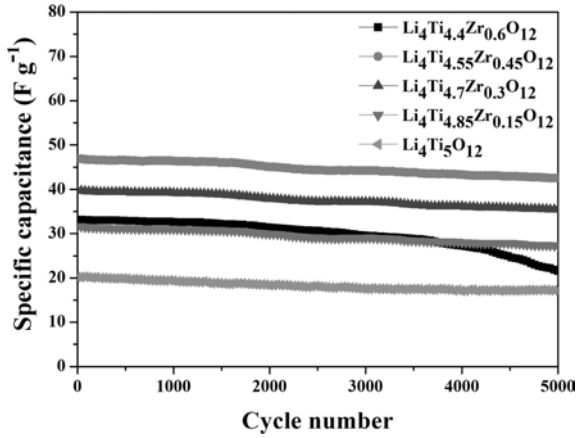

Fig. 5. Cycling performance of the hybrid supercapacitors using $Li_4Ti_{5-x}Zr_xO_{12}$ ($0 \le x \le 0.6$) anode materials at the rate of 2.5 Ag^{-1}.

original $Li_4Ti_5O_{12}$ structure.

The cyclic voltammetric (CV) curves of hybrid supercapacitor using the $Li_4Ti_{5-x}Zr_xO_{12}$ below $x = 0.6$ was measured in the range of 0 V to 2.8 V, show in Fig. 4. The supercapacitor shows the symmetric CV profile. This is called the mirror effect of rectangular shape [6]. However, hybrid supercapacitor shows the asymmetric CV shape [23]. Because the redox peak of Li-ion intercalation/deintercalation $Li_4Ti_5O_{12}$ is exhibited 2.3 V and 2.2 V, respectively, in the CV curves. The CV curves show a similar shape. The CV region of $Li_4Ti_{5-x}Zr_xO_{12}$ was expanded with increasing the Zr content. The reason is that the Zr doping effected on electrochemical reaction process of $Li_4Ti_5O_{12}$ anode. However, the CV area of $Li_4Ti_{4.4}Zr_{0.6}O_{12}$ was reduced above $x = 0.6$. The CV area of $Li_4Ti_{5-x}Zr_xO_{12}$ shows a trend corresponding to initial discharge capacitance in Fig. 3. The expanded lattice parameters by Zr doping improved the Li^+ diffusivity at intercalation/deintercalation.

Fig. 5 shows the result of a hybrid supercapacitor using at 2.5 Ag^{-1} up to 5,000 cycles performances. The cycling performance of $Li_4Ti_{5-x}Zr_xO_{12}$ with $x = 0.15$ and 0.45 improved compared with the pristine $Li_4Ti_5O_{12}$. The $Li_4Ti_{5-x}Zr_xO_{12}$ below $x = 0.6$ retained the specific capacitance which is appeared 84.6, 86.36, 89.25, 90.72 and 64.97%, respectively, after 5,000 cycles. Among them, the specific capacitance of $Li_4Ti_{4.55}Zr_{0.45}O_{12}$ exhibited the highest value. However, the specific capacitance of $Li_4Ti_{4.4}Zr_{0.6}O_{12}$ is lower than that of the $Li_4Ti_{5-x}Zr_xO_{12}$ with $x = 0.3$ and 0.45. Also, the specific capacitance of $Li_4Ti_{4.4}Zr_{0.6}O_{12}$ was decreased after 4,000 cycles rapidly. The hybrid supercapacitor using Zr doped $Li_4Ti_5O_{12}$ shows the superior structural stability. Also, the hybrid supercapacitor have high reversibility by the Zr doped $L_4Ti_5O_{12}$.

Conclusions

In this paper, the hybrid supercapacitor using $Li_4Ti_{5-x}Zr_xO_{12}$ ($0 \le x \le 0.6$) anodes were successfully fabricated. We studied the effect of Zr doped $Li_4Ti_5O_{12}$ on electrochemical performance of hybrid supercapacitor. The XRD patterns of $Li_4Ti_{5-x}Zr_xO_{12}$ ($0 \le x \le 0.45$) exhibited no secondary phases. This means that the original $Li_4Ti_5O_{12}$ structure was not deformed by Zr doping. This affected the electrochemical performance of hybrid supercapacitor because the expanded lattice parameters and improved conductivity enhanced the kinetics of Li-ion at anode. The $Li_4Ti_{5-x}Zr_xO_{12}$ (0x0.6) anode has bigger the CV area as compared with pristine $Li_4Ti_5O_{12}$ anode. Also, the $Li_4Ti_{4.55}Zr_{0.45}O_{12}$ anode has not only highest specific capacitance of 69 Fg^{-1} at 0.5 Ag^{-1} but also superior retention of 90.724% after 5000 cycles. However, the electrochemical performance of hybrid supercapacitor using $Li_4Ti_{4.4}Zr_{0.6}O_{12}$ anode decreased than that of the $Li_4Ti_{4.55}Zr_{0.45}O_{12}$ by deformation of $Li_4Ti_5O_{12}$. Therefore, the $Li_4Ti_{4.55}Zr_{0.45}O_{12}$ anodes can be expected to use as superior anode in the various energy storage devices.

Reference

1. S. H. Lee, S. G. Lee, J. R. Yoon, H. K. Kim, J. Power Sources 273 (2015) 839.

2. Seung-Hwan Lee, Hong-Ki Kim, JeongHyun Lee, Sung-Gap Lee, Young-Hie Lee, Materials Letters 143 (2015) 101.
3. Ting-Feng Yi, Li-JuanJiang, J. Shu, Cai-Bo Yue, Rong-Sun Zhu, Hong-Bin Qiao, Journal of Physics and Chemistry of Solids 71 (2010) 1236.
4. K. Naoi, S. Ishimoto, Y. Isobe, and S. Aoyagi, *J. Power Sources* 195, 6250 (2010).
5. Li Li Zhang and X. S. Zhao, Chem. Soc. Rev. 38 (2009) 2520.
6. Hong-Qiang Wang, Ze-Sheng Li, You-Guo Huang, Qing-Yu Li and Xin-Yu Wang, J. Mater. Chem. 20 (2010) 3883.
7. Yong-gang Wang, Yong-yao Xia, Electrochemistry Communications 7 (2005) 1138.
8. Xing Li, Meizhen Qua, Yongjian Huaia, Zuolong Yua, Electrochimica Acta 55 (2010) 2978.
9. Y. Zhao, S. Pang, C. Zhang, Q. Zhang, L, Gu, X. Zhou, G. Li, and G. Cui, J. Solid State Electrochem. 17 (2013) 1479.
10. Chenguang Liu, Zhenning Yu, David Neff, Aruna Zhamu, and Bor Z. Jang, Nano Lett. 10 (2010) 4863.
11. Byung Gwan Lee, and Jung Rag Yoon, Journal of Electrical Engineering & Technology 7 (2012) 207.
12. T. F. Yi, B. Chen, H. Y. Shen, R. S. Zhu, A. N. Zhou, and H. B. Qiao, *J. Alloys Comp.* 558 (2013) 11.
13. H. G. Jung, N. Venugopal, B. Scrosati, And Y. K. Sun, *J. Power Sources* 221 (2013) 266.
14. B. Zhang, H. Du, B. Li, and F. Kang, Electrochem. Solid-State Lett. 13 (2010) A36.
15. T. F. Yi, Y. Xie, Q. Wu, H. Liu, L. Jiang, M. Ye, and R. Zhu, J. Power Sources 214 (2012) 220.
16. Hun-Gi Jung, Chong Seung Yoon, Jai Prakash, and Yang-Kook Sun, J. Phys. Chem. C 113 (2009) 21258.
17. G. Du, N. Sharma, V. K. Peterson, J. A. Kimpton, D. Hia, and Z. Guo, Adv. Funct. Mater. 21 (2011) 3990.
18. J. Gao, J. Ting, C. Jiang, and C. Wan, *Ionics* 15 (2009) 597.
19. X. Li, M. Qu, and Z. Yu, *J. Alloys Comp.* 487 (2009) L12.
20. Haiying Yu, Xianfa Zhang, A.F. Jalbout, Xuedong Yan, Xiumei Pan, Haiming Xie, Rongshun Wang, Electrochimica Acta 53 (2008) 4200.
21. E. M. Sorensen, S. J. Barry, H. K. Jung, J. M. Rondinelli, J. T. Vaughey, and K. R. Poeppelmeier, Chem. Mater. 18 (2006) 482.
22. Z. Yu, X. Zhang, G. Yang, J. Liu, J. Wang, and R. Wang, J. Zhang, Electrochim. Acta 56 (2011) 8611.
23. S. H. Lee, H. K. Kim, Y. S. Yun, J. R. Yoon, S. G. Lee, and Y. H. Lee, Int. J. Hydrogen Energy 39 (2014) 16569.